Environmental Impact Assessment (EIA) of pH and Other Factors on Organic Photovoltaic Performance Output

Abodunrin Temitope Jolaolu[1], Emetere Moses Eterigho[1] and Ajayi Oluseyi Olanrewaju[2]
[1]*Department of Physics, Covenant University, P.M.B. 1023, Ota, Nigeria*
[2]*Department of Mechanical Engineering, Covenant University, P.M.B. 1023, Ota, Nigeria*

[*]*corresponding author email address*

Keywords: Dye-sensitized Solar Cell, Impact Assessment, Energy, pH.

Abstract: A methodical frame for evaluating the prospective ecological and health impacts of photovoltaics is necessary to consider both their negative and positive underlying effects. These pros come with a probability to advance carbon sequestration perspective. The cons are considered with a view to alleviate their negative consequences or eliminating them altogether. In this work, we report the effect of pH and dye sol ambient temperature on the environmental impact of three dye-sensitized solar cells, *C.papaya*, *P.dulcis* and *C.longa* to gauge their environmental impact. In the wake of several generations of photovoltaic trends a precautionary check on their effectiveness, stability, cost-competitiveness, storage time and ecological friendliness is a way of isolating carbon for storage and transportation. Thus, although the objective of this project is to investigate factors which are not tangible, discrete factors that impact photovoltaics will be analyzed using direct qualitative techniques. Using valued environmental components with spatial boundaries, and software effort estimation model to investigate the possibility for re-use, compactness and photo-corrosion among others. The significance of this research is for subsequent moderation in planning, design and to redress newer models of dye-sensitized solar cells technology for higher photovoltaic efficiency and lessen their photo-corrosive influence on our ecological system.

1 INTRODUCTION

In the wake of so many hazardous emissions released per second into the atmosphere from myriad industrial and economical activities, it is imperative to carry out a risk assessment on many of our research efforts. This is in particular so because of the dimensions of the changes involved; at the moment, industry, transportation, and domestic uses routinely discharge almost 10 Giga tons of carbondioxide yearly to the atmosphere. It is equally notable that there is no immediate hope for a radical change in the spate of these emissions (Abdullahi *et al*., 2018). Thus, a clarification of carbon sequestration and carbon 'sink' needs to precede many of our lines of research intervention. A carbon sink accumulates more and more carbon into the atmosphere or ocean whereas, a sequestrate serves as a carbon reservoir. This artificial storage acts as a check for increasing the atmospheric carbondioxide (Smit *et al*., 2014). Real life scenario requires more cyclable carbon reservoirs as fuel which readily get replenished as they combust in oxygen to generate energy. In the present circumstance, such a store should not act as a trigger for global warming or its associative epidemic hazardous effects. Consequently, calculation of the risk involved in installation of any photovoltaic becomes a standard measure of probability of any harmful effects, such as its propensity for 'carbon sink or store'. The process of trapping and storing carbondioxide as a means of decreasing its volume in the atmosphere and mitigating climatic change is defined as sequestration of carbon (Lal *et al*., 2013). Inadvertently, there are natural carbon sequestration processes but, that due to anthropogenic actions of man leads to accruement of carbon dioxide in the atmosphere. This follows up on carbon footprint and is understandably a rising cause for concern in climate issues (Park *et al*., 2011). Photovoltaics use redox reactions, this by implication suggests innate balance but, the nature of certain materials used within their components reveals the contrary. An illustration of electrolytes used is: leaky, volatile compounds, corrosive or toxic liquids, this forms the

Jolaolu, A., Eterigho, E. and Olanrewaju, A.
Environmental Impact Assessment (EIA) of pH and Other Factors on Organic Photovoltaic Performance Output.
DOI: 10.5220/0009782501590168
In *Proceedings of the 9th International Conference on Smart Cities and Green ICT Systems (SMARTGREENS 2020)*, pages 159-168
ISBN: 978-989-758-418-3

epic of our environmental quest (Martelli *et al*., 2011). Incorporation of a photoanode usually involves cataclysmic reactions with concentrated acid, pungent gases are emitted in the vicinity, this brings a second perspective on the environment (Olateju and Kumar, 2013). Preparation of the counter electrode through masking it with platinum or other carbon-based compounds is also an obvious intrusion of carbon into the atmosphere (Botero *et al*., 2013). It thus poses a high-level risk if photovoltaics become a significant source of carbon source sink, which has informed this research - a prospect of orchestrating more collective carbon detention and storing from improved changes in photovoltaic fabrication and application techniques (Wich *et al*., 2020). One of the greatest milestones of this century is a need to stabilize the greenhouse gas concentrations of the atmosphere (Müller *et al*., 2020). To regulate these gaseous discharges, human race can either lessen fossil fuel emissions directly or diagnose instruments to get rid of greenhouse gases once they are emitted (Heek *et al*., 2018). In this way, sequestration of atmospheric carbon dioxide becomes an appealing option as a substitute to help truncate the astronomical rate of greenhouse gases and accompanying changes to climate patterns. A priority factor for consideration in this ecological theme is reusability, it is difficult to sustain any technology without any possibility for reuse (Ani and Basri, 2013). In order to carry out an effective valuation, a program software will have been used. Although many algorithms have played dual or more roles in past researches whether applied individually or corporately, many more are ongoing to unravel the scientific facts embedded in present and future numerical data (Bettinger *et al*., 2017). A search for suitable software suited to the demands of this particular research led to environmental impact assessment (EIA). This is because, it was initially written as a software programming tool established to scale environmental impact of human activities on the environment (Amundson and Biardeau, 2018). Consequently, modification of EIA comes to play in prior assessment of the effect of fabrication of dye-sensitized solar cell on the environment with a view of taking better decisions (Broday, 2020). This begins with prior collection of data on the manufacturing process, different stages of completion ranging from scope to completion governed by EIA tool with a determination to improve on the present by exploring even safer and better alternatives (Zeleňáková et al., 2020). Comprehensively, many research works have focused on the effect of pH, because altering the pH level in any ecosystem affects all living organisms (Barandiaran and Rubiano-Galvis, 2019). There are very few highlights on hazard footprints with specific mention of vulnerability resulting from concentrated acid interactions with titanium oxide as a naturally-induced hazard which is another factor considered for quantification of the afore-mentioned risk factors (Wang and Su, 2020). The expected outcome is higher Quality photovoltaics even with onset of time, solvent deals in which neither sol gel gets evaporated nor washed off by degeneracy, cleaner air quality from cost-effective photovoltaic devices.

2 METHODOLOGY

Stoichiometric quantities of *C.papaya*, *P.dulcis* and *C.longa* plants were air dried under conditions of standard air mass in the laboratory. Their dried extract was mixed in (5mg/5ml) methanol proportion, the pH and temperature of each sample was recorded before being affixed onto three separate titanium frameworks already assembled on the indium doped (ITO) conducting slides following standard procedures described in previous researches (Abodunrin *et al*., 2019). This procedure describes the photoanode preparation, the counter electrode comprised of masking a second pair of ITO with co-axial deposition of soot over a naked flame, in a simulated vacuum-like enclave. Each pair of anode and counter electrode was fastened together with clips, 5ml syringes were used to insert three drops of aqueous electrolyte in-between the resultant ITO sandwich. Excess electrolyte was allowed to tun off but was noted for subsequent assessment in the ensuing section. Each pair of ITO were connected in parallel to a multimeter and variable resistive load with the aid of flexible connecting wires to obtain photovoltaic parameters (Abodunrin *et al*., 2019). Experimental values of short circuit (I_{sc}), open circuit voltage (V_{oc}), maximum power (P_{max}), fill factor (*ff*) and efficiency are the measurements taken. The experimental set-up was taken outdoors and exposed to conditions of standard airmass of 760mmHg. The indoor air quality due to concentrated nitric acid blended to a colloidal paste with titanium oxide during preparation, calcination and subsequent fabrication was determined by assigned values consistent with EIA averages. The pH of the dye sol of each dye was determined with using a pH meter and the temperatures were recorded. In addition, phytochemical screening of the extracts identified the chromophores present in each dye (Abodunrin *et al*., 2019). The Fourier Infrared spectroscopy of each dye would be used to study the strong reactions and their

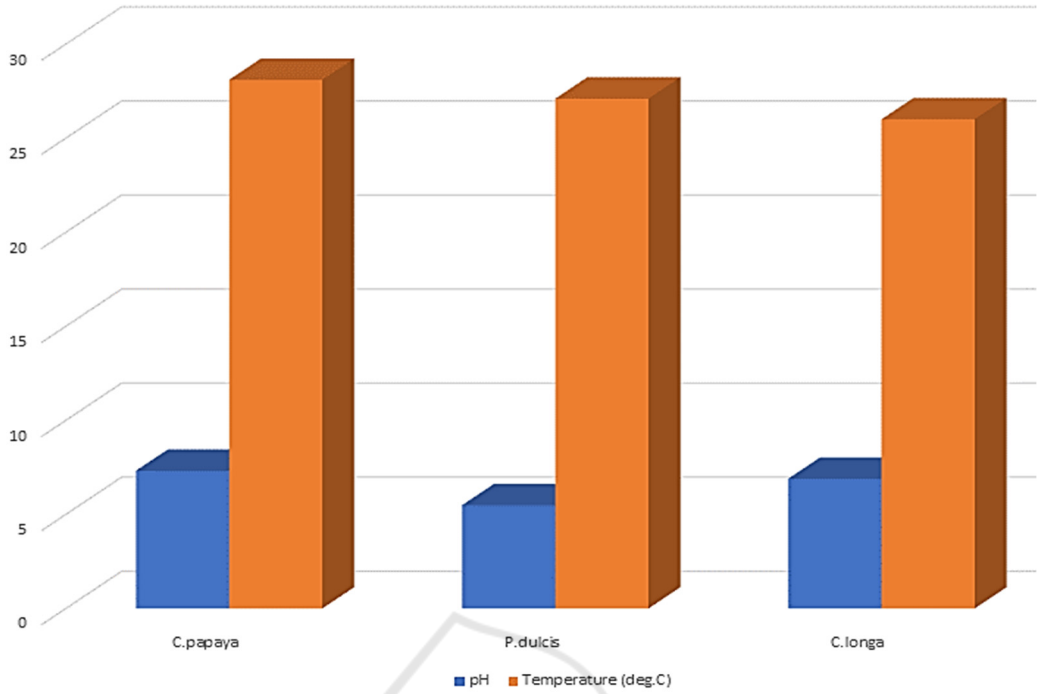

Figure 1: Comparison of pH and temperature of three organic extracts.

possible consequent emissions into the environment. Detailed analysis of their performances relative to images from modelling their scanning electron micrographs was used to obtain vital statistics for computation of EIA.

3 RESULTS AND DISCUSSION

The pH and temperature of the three organic dyes are as presented in Figure 1. *P.dulcis* dye records the least value in temperature, 27.1°C. This is closely followed by *C.longa* with a value of 27.8°C and the relative highest temperature reading is given by *C.papaya* with a temperature of 28.1°C. The average normal surrounding temperature is 27°C, *P.dulcis* is the nearest in ambient temperature while *C.papaya* is the farthest in this context. The Environmental Complexity factor is calculated as shown in Equations 1-4 (Ani and Basri, 2013).

3.1 List of EIA Equations

$$ECF = 1.4 + \left(-0.3 \times E_{factor}\right) \quad (1)$$

$$TCF = 0.6 + \left(0.01 \times T_{factor}\right) \quad (2)$$

$$UUCP = UUCW + URW \quad (3)$$

$$UCP = UUCP + (TCF \times ECF) \quad (4)$$

Where *ECF* is the Environmental Complexity Factor, *TCF* represents Technical Case Factor, *UUCP* denotes the unadjusted Use Case Point, *UCP* connotes the Use Case Points and *URW* is Unadjusted Reaction Weight.

3.1.1 Environmental Complexity Factor (ECF)

Higher values of environmental factor imply greater impact on the UCP equation. Thus, assigned value of one implies the factor has a weak impact in this venture, two is average while three signifies a strong impact. This means that zero-value is of no consequence on the environment. For example, temperature of *P.dulcis* would be assigned 0.1, *C.longa* would be given 0.8 while *C.papaya* is given 1.1. In addition, pH of *C.papaya* is 7.32, this is a little above neutral on the Universal indicator scale hence, its value would be 0.32. *C.longa* has a pH of 6.90, the impact would be slightly negative on the environment, it is assigned a value of -0.1 and *P.dulcis* has a value of 5.49, this is even more negative due to its acidity. It is assigned a value of -

1.51 while in this context basicity of an alkaline dye would be assigned positive values. Another factor that contributes to negatively to the environment are the drops of electrolyte introduced in-between each dye cell to facilitate charge transport. The cumulative effect is accorded a value or weight comprising of the sum of its ambient temperature factor with the pH factor multiplied by its apparent impact to yield its calculated impact factor. The calculated factors are added together to produce the Environmental factor as shown in Table 1.

Table 1: Break down of ECF parameters.

Factor	Dye	Weight	Assessment	Impact
E_1	*C.papaya*	1.1+0.32 =1.42	3	4.26
E_2	*P.dulcis*	0.1-0.10 = 0	3	0
E_3	*C.longa*	0.8-1.51 = 0.71	3	-2.13
			Total E_{factor}	-2.13

3.1.2 Technical Complexity Factors (TCF)

Arbitrary values between 0 to 3 are assigned subjectively. The factors revolve around re-use, and recycle viability. Responses for each application that has a high influence like efficiency, 3 is awarded. The higher the efficiency, the more viable it becomes in its universal adoption. Response time infers how fast the device responds to the required stimulus of operation as this is paramount, it is allotted 3. Kinematics refers to the excitation state of the reactants in a dye-sensitized solar cell, whether their momentum is elastic and the principle of conservation of energy and linear momentum is conserved. This decides the equilibrium of the reaction, either the forward or backward reaction is occurring and when they nullify to reverse each other. Portability is the degree of compactness and ease of transporting the device which is a prerequisite to the realization in the primary function of any photovoltaic. A bulky photovoltaic would experience transportation challenges and limitation in its universal adoption. The output efficiency is directly associated to the photovoltaic performance of each dye-sensitized solar cell. A zero is given to any factor that does not have any influence on the study. A midpoint value of 2 is assigned to factors that are neither so strong yet have a measure of influence on this study. Individual factor's weight is multiplied by its perceived complexity factor to give a resultant calculated factor. The calculated factors are summed to produce the Total Technical Factor.

Table 2: Technical Factors of EIA.

Factor	D	Wt	Assessment	Impact
T_1	Response Time	3	3	9
T_2	End user Efficiency	0	1	0
T_3	Kinematic of Reaction	2	3	6
T_4	Reusability	1	0	0
T_5	Usability	3	3	9
T_6	Portability	1	2	2
T_7	Output Efficiency	3	3	9
			Total T_{Factor}	35

Key: D stands for Description, Wt connotes Weight

3.1.3 Phytochemical Result in Terms of EIA

The outcome of phytochemical screening of the three dyes is as shown in Table 3. A phytochemical screening refers to the process of extracting, identifying the bioactive substances such as: antioxidants, flavonoids, tannins and so on. Presence of any phytoconstituent is assigned a value of 1, while its absence has no value and is given zero. The significance of phytochemicals in dye-sensitized solar cells is that, they contribute to the ionic radical available for the redox reaction. It implies that, the measure of effectiveness in a dye-sensitized solar cell is a direct consequence of the metabolites available in its bio-constituents. They also provide necessary immunity for preserving the life cycle of the dye-sensitized solar cell throughout. Hence the UUCW is calculated from the product obtained from the number of phytochemicals, weight and the number of cases as shown in Table 4. In this project, loss of potency in the phytochemical constituents is not given a consideration such as the absorbance in the UV/Vis region over a period of time. Thus, by tacit agreement the electrolyte activates the dye-sensitized solar cell whenever it is in operation. Furthermore, since each phytochemical assist in the electrochemical equilibrium, each is awarded the same strength, a value of unity.

Table 3: Phytochemicals in organic extracts.

	Ch	Ta	Sa	Fl	Al	Qu	Gl	Ca	Te	Ph	St
C.p	+	-	+	+	+	-	-	+	-	+	-
P.d	-	+	+	+	+	-	-	+	-	+	-
C.l	+	-	+	+	+	-	-	+	-	-	-

Key: Ch (CHO); Ta (Tannin); Sa (Saponin); Fl (Flavonoid); Al (Alkaloid); Qu (Quinone); Gl (Glycoside); Ca (Cardiac Glycoside); Te (Terpenoid); Ph (Phenol); St (Steroid); + indicates presence, - means absence

C.p represents *C.papaya*, *P.d* stands for *P.dulcis*, *C.l* represents *C.longa*

The significance of this result is that, with respect to their electrochemical index, *C.longa* < *C.papaya* = *P.dulcis* as indicated on Table 4. Relating this to the ECF, the electrolyte in *C.longa* would require more energy to raise the Fermi potential for excitation. Hence, the negative impact of -2.13.

Table 4: Phytochemicals in terms of UUCW.

Use case complexity	Number of phytochemicals present	Wt	Number of use cases	Pdt
C.papaya	6	1	11	66
P.dulcis	6	1	11	66
C.longa	5	1	11	55
			Total UUCW	187

Key: Wt represents Weight, Pdt stands for Product

3.1.4 Unadjusted Reaction Weight (URW)

The appearance of each functional group in a Fourier Infrared Spectrograph is a characteristic that distinguishes it from others in a chemical reaction as shown in Appendix I. In effect, each property identified is assigned a weight: -1 is given to the unidentified wavelength frequencies, 1 is assigned to the weak (*w*) intensity, *m* is allotted 2 for medium intensity while

3, 4 and 5 is given to strong (*s*), strong – narrow (*s,n*) and strong -broad (*n,s*) intensities respectively. Their occurrences connote the number of times they appear, the product symbolizes their cumulative frequency. The significance of the strength of reaction determines the direction of the kinematics of the overall dye-sensitized solar redox reaction and the Fermi level in the photovoltaic.

Table 5: FTIR of *P.dulcis* dye.

P.dulcis		
Wavelength	Functional Group	Intensity
3423.76; 2926.11; 2852.84	O-H stretching	*s,b*
2426.53	Unidentified	
2085.12	CO_2 stretching	*s*
1741.78	C=O stretching	*s*
1658.84; 1608.69	C=C stretching in alkene di-substitution	*w*
1498.74	Unidentified	
1456.30	Unidentified	
1384.94; 1346.36; 1298.14; 1253.77; 1207.48; 1182.40; 1084.03; 1043.52	O-H bending in carboxylic acid	*m*
931.65	Unidentified	
842.92;715.61; 642.32; 574.81	C-Cl stretching in alkyl halides	*s*
522.73;	Unidentified	

s: strong; *w*: weak; *n*: narrow; *m:* medium; *b*: broad

Table 6: FTIR of *C.longa*.

C.longa		
Wavelength	Functional Group	Intensity
3853.90; 3421.83	O-H stretching	*s, b*
2926.11; 2852.81	Acid O-H	*s, n*
2426.53	O-H stretching	*w*
2285.72; 2085.12	O=C=O in CO_2	*s*
1741.78; 1658.84	C-H bending in aromatics	*W*
1608.69	C=C stretch in alkene disubstituted	*w*
1498.74; 1456.30	C-C stretch in ring aromatics	*m*
1384.94; 1346.36	Symmetric nitro compounds	*m*
1298.14; 1253.77; 1207.48; 1182.40	Acyl stretching	*s*
1084.03; 1043.52	C-O stretching in Alkoxy	*m*
931.65	Unidentified	
842.92	C-Cl stretching in alkyl	*s*
715.61; 642.32	Meta di-substituted C-H bend	*w*
574.81; 522.73	C-Br Stretching in alkyl	*s*
424.35	Unidentified	

Key: *s*: strong; *w*: weak; *n*: narrow; *m:* medium; *b*: broad

Table 7: FTIR of *C.papaya.*

C.papaya		
Wavelength	Functional Group	Intensity
3429.55; 2926.11	N-H stretching in 2º amine	*s*
2854.74	C-H stretching	*m*
2729.37; 2507.54	O-H stretching in carboxylic acid	*s,b*
2019.54	Unidentified	
1735.99; 1637.62	C-H bending	*w*
1458.23	Unidentified	
1377.22; 1244.13; 1168.90; 1072.46; 1037.74	C-F stretching in Fluoric compounds	*s*
873.78	C=C bending in alkene di-substituted	*w*
839.06; 723.33; 665.46	C-Cl stretching in alkyl compounds	*s*
597.95; 515.01	C-Br stretching in alkyl compounds	*w*
437.86	Unidentified	

Table 8: FTIR of dyes in terms URW.

Dye	Weight				Occurrences				Pdt
P.d	*S*	*m*	*w*	*U*	*s*	*m*	*w*	*U*	
	3-5	2	1	-1	3,0,1	2	1	4	15
C.l	*S*	*m*	*w*	*U*	*s*	*m*	*w*	*U*	
	3-5	2	1	-1	4,1,1	3	4	2	29
C.p	*S*	*m*	*w*	*U*	*s*	*m*	*w*	*U*	
	3-5	2	1	-1	3,0,1	1	3	3	16
								URW_{Total}	60

C.p represents *C.papaya*, *P.d* stands for *P.dulcis*, *C.l* represents *C.longa*

3.1.5 Stereochemistry of Dyes on EIA

The interpretation of the dye molecular structure with regards to their atomic position in 3-dimensional space is required for the EIA. Thus, the phytochemicals will be investigated for their reaction in the applied photovoltaic. In particular, carbohydrate presence would be examined as illustrated in Figure 2.

The chemical formula differs from the characteristic $C_6H_{12}O_6$ due to the chemical reaction in the photovoltaic. Element composition conforms with the standard CHO in organic compounds, in effect these elements have a positive photo degeneracy quotient.

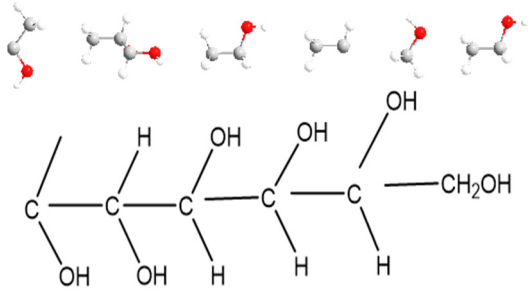

Chemical Formula: $C_{12}H_{30}O_6$
Exact Mass: 270.20
Molecular Weight: 270.37
m/z: 270.20 (100.0%), 271.21 (13.0%). 272.21 (1.2%)
Elemental Analysis: C, 53.31; H, 11.18; O, 35.51

Figure 2: Analysis of Carbohydrate in dyes.

It is pertinent to also explore the sole presence of tannins in *P.dulcis*, the reaction interpretation is as shown in Figure 3. The presence of tannins influenced the unadjusted reaction weight (URW) to give the least value. It is also noteworthy that, tannins probably assisted *P.dulcis* in actualizing the zero impact on the environmental complexity factor (ECF). This is attributable to its numerous ligands which facilitate its articulation with other bio-molecules. Hence, it has better photo degeneracy than Carbohydrates.

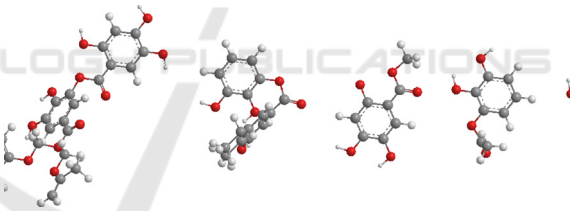

Chemical Formula: $C_{61}H_{65}O_{29}$
Exact Mass: 1261.36
Molecular Weight: 1262.16
m/z: 1261.36 (100.0%), 1262.36 (66.0%), 1263.37 (21.4%), 1263.37 (6.0%), 1264.37 (4.6%), 1264.37 (3.9%)
Elemental Analysis: C, 58.05; H, 5.19; O, 36.76

Figure 3: Analysis of Tannin in *P.dulcis* dye.

The presence of flavonoid in all three organic dyes makes available bio-catalysts in the respective photovoltaic reactions. It also offers a large store of carbon atoms from the C_6-C_3-C_6 molecular framework. The three organic photovoltaic cells act as a form of carbon sequestrate as shown in Figure 4.

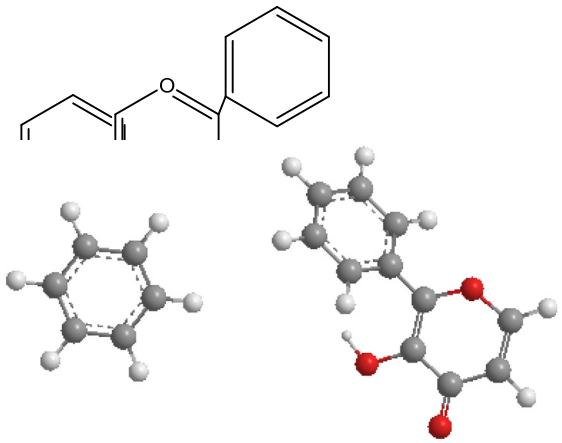

Chemical Formula: $C_{17}H_{14}O_3$
Exact Mass: 266.09
Molecular Weight: 266.30
m/z: 266.09 (100.0%), 267.10 (18.4%), 268.10 (1.6%)
Elemental Analysis: C, 76.68; H, 5.30; O, 18.02

Figure 4: Interaction of Flavonoid in dyes.

The interaction of saponins in the three photovoltaic cells will be considered in order to assess the environmental impact. Saponins provide the underlying foundation for the assortment of functional groups attachment and determines the general shape of the molecule. Saponins serve a steroidal physiological function keeping the other bio-substances active. Their ligands combine with other functional groups during the chemical reaction in the photovoltaic as shown in Figure 5.

Chemical Formula: $C_{37}H_{72}$
Exact Mass: 516.56
Molecular Weight: 516.98
m/z: 516.56 (100.0%), 517.57 (40.0%), 518.57 (7.8%)
Elemental Analysis: C, 85.96; H, 14.04

Figure 5: Analysis of Saponin Effect on Photovoltaic.

Interestingly, the phenolic ring is a recurrent feature in both saponins and flavonoids. A third consistent functional group in the dyes is the Alkaloid. Phenols constitute the major class of secondary metabolites in plants. Their aromatic nature is responsible for pigmentation, flavour (not applicable in this study) and acerbity. Although they possess -OH functional group similar to alkaloids, they exhibit stronger potency in chemical reactions.

These interactions with the concentrated trioxonitrate (V) acid and titanium will be discussed with a focus on their EIA impact. The energy and gradient of applying the concentrated trioxonitrate (V) acid on the titanium was run with CHEM DRAW and the output is as shown in Figure 6.

HNO3

Figure 6: A model of Concentrated HNO_3.

The Energy (MMFF94) and Gradient was determined using software program estimate. The total energy for this frame was given as, 15.976 kcal/mol. The RMS Gradient was given as 44.260. Thus, the MM2 Calculation completed successfully.

The MM2 Dynamics was obtained from Pi System: 5 4 6.

Some parameters are assigned (Quality = 1). The remaining associated properties were calculated and the result is as shown on Table 9.

Table 9: Dynamics of Reaction.

Stretch	4.6807
Bend	3.1011
Stretch-Bend	-0.2023
Torsion	-0.5171
Non-1,4 VDW	-0.0943
1,4 VDW	2.2077
Charge/Charge	0.0000
Charge/Dipole	-5.7107
Dipole/Dipole	6.3333

The total energy for this frame: 9.799 kcal/mol
The energy of the reaction was the second value determined, in this context of the photovoltaic reaction and the environmental impact.

The Equations of the redox reaction in the photovoltaic cells is as indicated in Equations 5-7 (Cadien and Nolan, 2012). The dye (D) absorbs photons of energy from the sun and becomes excited D^*as shown in Equation 5, the dye is affixed to the titanium frame. The oxidized or excited dye gets reduced by iodide as illustrated in Equation 6. The

formation of iodide radical on the oxide surface is shown in Equation 7.

$$TiO_2/D + hv \rightarrow TiO_2/D^* \quad (5)$$

$$TiO_2/D^* + 2I^- \rightarrow TiO_2/D + I_2^- \quad (6)$$

$$2I_2^- \rightarrow I^- + I_3^- \quad (7)$$

The effect of concentrated nitric acid on the environment is shown in the Appendix. The graph illustrates a sine crest, depicted by an initial rise in the density of the molecules of the acid as it reaches a peak. As diffusion occurs with air molecules colliding with the fumes given off from the acid, the peak gradually slopes down until there is equilibrium.

4 CONCLUSIONS

Environmental Complexity Factor (ECF) from Equation 1 gives 2.639, Technical Complexity Factor gives 0.95 from Equation 2, Unadjusted case product in Equation 3 is given as 247, Use Case Point from Equation 4 gives 421.55 in 2 decimal places. It is generally difficult to gauge the environmental effect based on this outcome unless there is a standard for comparison. Hence, at this point it is imperative to introduce an index. The first is a comparison of each dye relative to the sum-total of the effect of all the dyes. On this basis, individual assessment for the dyes give 8.544, 8.468 and 15.68 for *C.papaya*, *P.dulcis* and *C.longa* respectively. *C.longa* dye has close to the addition of the individual effects of *C.papaya* and *P.dulcis* dyes. This is a direct consequence of the unadjusted reaction weight (URW) factor. Converse to conventionality, this project reveals that all organic dyes have an effect on the environment, although their impact varies for different photovoltaics. Another salient factor becomes measuring the level of impact, in terms of photo degeneracy relative to fossil fuels. In terms of degradation, each organic dye produces negligible effect but the combination of dyes has a multiplicity effect on the environment which is minimal with respect to fossils. *C.longa* has almost double the environmental footprint of *C.papaya* and *P.dulcis* as indicated in this result. The photo degeneracy of *C.longa* is double in its consequence. In terms of the FTIR spectroscopy, *C.longa* shows CO_2 at two wavelength frequency peaks, *C.papaya* shows in just one, *P.dulcis* shows none. This is a direct consequence of their carbon sequestration characteristic, *P.dulcis* is not a carbon sequestrate. Eventually, this study shows a direct correlation between the environmental footprint of the dyes through their CO_2 reaction. In terms of carbon sequestration, *C.longa* dye is determinedly the best of all three dyes in ultimately reducing the greenhouse effect.

The outcome of this project prescribes the following measures:

1. The environmental footprint of dyes should be one of the foundational studies carried out before their subsequent use in photovoltaics.
2. A preliminary information on Fourier Infrared spectroscopy of any extract should be a prerequisite source of information on the reaction that each dye content would promote.
3. Promoting the natural photovoltaic processes is a simple but effective means of reducing the atmospheric carbondioxide levels. This is because, dispersed carbondioxide sources are very challenging to harness for cost effective carbon separation and capture methods.

ACKNOWLEDGEMENTS

The authors of this work are immensely grateful to Covenant University for providing an appropriate ambience required for the investigation of this research. They also wish to appreciate the technologists at the Chemistry department of Redeemers' University, Ede for the Fourier Infrared spectroscopy of the organic dyes. Their gratitude goes to the technologists at the Biochemistry laboratory of Covenant University for their expertise in identifying the phytochemicals present in each of the dye.

REFERENCES

Abdullahi, A.C., Siwar, C., Shaharudin, M.I., Anizan, I. J., 2018. Carbon Sequestration in Soils: The Opportunities and Challenges. *Intechopen*, 79347.

Smit, B., Reimer, J.A., Oldenburg, C.M., Bourg, I.C., 2014. Introduction to Carbon Capture and Sequestration. *The Berkeley Lectures on Energy*, 1: 596.

Lal, R., Lorenz, K., Hüttl, R.F., Schneider, B.U., von Braun, J., 2013. Ecosystem Services and Carbon Sequestration in the Biosphere. *Springer Books*: 467.

Park, S.K., Ahn, J.H., Kim, T.S., 2011.Performance evaluation of integrated gasification solid oxide fuel cell/gas turbine systems including carbon dioxide capture. *Applied Energy*, 88(9): 2976-2987.

Martelli, E., Kreutz, T., Carbo, M., Consonni, S., Jansen, D., 2011. Shell coal IGCCS with carbon capture:

Conventional gas quench vs. innovative configurations. *Applied Energy*, 88(11): 3978-3989.

Olateju, B., and Kumar, A. 2013.Techno-economic assessment of hydrogen production from underground coal gasification (UCG) in Western Canada with carbon capture and sequestration (CCS) for upgrading bitumen from oil sands. *Applied Energy*, 111: 428-440.

Botero, C., Field, R.P., Herzog, H.J., Ghoniem, A.F., 2013. Impact of finite-rate kinetics on carbon conversion in a high-pressure, single-stage entrained flow gasifier with coal–CO_2 slurry feed. *Applied Energy*, 104: 408-417.

Wich, T., Lueke, W., Deerberg, G., Oles, M., 2020. Carbon2Chem®-CCU as a Step Toward a Circular Economy. *Frontiers in Energy Research*, 7: 162.

Müller, L.J., Kätelhön, A., Bachmann, M., Zimmermann, A., Sternberg, A., Bardow, A., 2020. A Guideline for Life Cycle Assessment of Carbon Capture and Utilization. *Frontier in Energy Research*, 8:15.

Heek, J.O., Arning, K., Linzenich, A., Ziefle, M., 2018. Trust and Distrust in Carbon Capture and Utilization Industry as Relevant Factors for the Acceptance of Carbon-Based Products. *Frontier in Energy Research*, 6: 73.

Ani, Z.C., Basri, S., 2013. A Web-Based Tool Support for Automating Software Effort Estimation. *Information Systems International Conference (ISICO).*

Bettinger, P., Boston, K., Siry, J.P., Grebner, D.L., 2017. *Forest Management and Planning,* Academic Press, 2nd edition.

Amundson, R., and Biardeau, L., 2018. Opinion: Soil carbon sequestration is an elusive climate mitigation tool. *Proceedings of the National Academy of Sciences of the United States of America*, 115 (46): 11652-11656.

Broday, D., Dayan, U., Aharonov, E., Laufer, D., Adel, M., 2020. Emissions from gas processing platforms to the atmosphere-case studies versus benchmarks. *Environmental Impact Assessment Review*, 80: 106313.

Zeleňáková, M., Labant, S., Zvijáková, L., Weiss, E., Čepelová, H., Weiss, R., Jitka Fialová, J., Minďaš, J., 2020. Methodology for environmental assessment of proposed activity using risk analysis. *Environmental Impact Assessment Review*, 80: 106333.

Barandiaran, J., Rubiano-Galvis, S., 2019. An empirical study of EIA litigation involving energy facilities in Chile and Colombia. *Environmental Impact Assessment Review*, 79: 106311.

Wang, Q., Su, M., 2020. Drivers of decoupling economic growth from carbon emission – an empirical analysis of 192 countries using decoupling model and decomposition method. *Environmental Impact Assessment Review*, 81: 106356.

Abodunrin, T.J., Emetere, M.E., Ajayi, O.O., Uyor, U.O., Popoola, O., 2019. Investigating the prospect of micro-energy generation in S. Anisatum Dye-sensitized solar cells (DSCs). *Journal of Physics: Conference Series*, 1299 (1): 012028.

Abodunrin, T. J., Boyo, A. O., Usikalu, M. R., Ajayi, O. O., 2019. Investigation of effect of batch-separation on the micro-energy generation in *M.indica L.* dye-sensitized solar cells. *Procedia Manufacturing*, 35: 1273-1278.

Abodunrin, T.J., Boyo, A.O., Usikalu, M.R., Emetere, M.E., 2019. Investigating the Influence of Selective Co-sensitization of Two N719 Dyes on the Micro-Energy Generation from Dye-sensitized Solar Cells. Journal of Physics: Conference Series 1299 (1), 012027.

Cadien, K.C., Nolan, L., 2012. CMP Method and Practice in Handbook of Thin Film Deposition, Science Direct, 3rd Edition.

APPENDIX

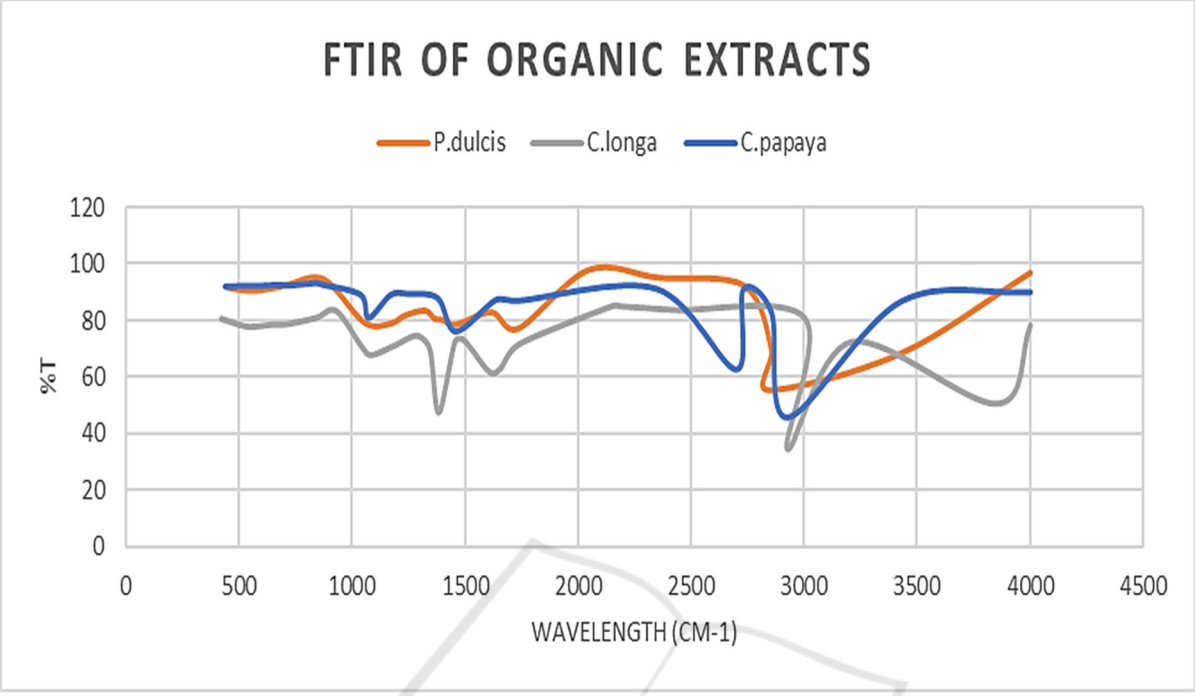

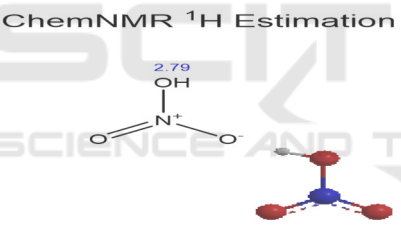

Estimation quality is indicated by color: good, medium, rough


```
Protocol of the H-1 NMR Prediction (Lib=SU Solvent=DMSO 300 MHz):

Node      Shift     Base + Inc.    Comment (ppm rel. to TMS)
OH   2.79                4.20       alcohol
                             ?         1 unknown substituent(s)
                          -1.41        general corrections

1H NMR Coupling Constant Prediction
shift    atom index   coupling partner, constant and vector
2.79          4
```